

# A novel pH-sensitive ceramic-hydrogel for biomedical applications<sup>†</sup>

Gabriel Goetten de Lima<sup>a</sup>, Lucas Campos<sup>a</sup>, Amanda Junqueira<sup>a</sup>, Declan M. Devine<sup>a,b</sup> and Michael J. D. Nugent<sup>a\*</sup>

**Innovations on the field of smart hydrogels are now being held with loads of advantages. With recent progress, smart polymers can now be used on the market for specific target/objectives desired on medicine. However, the field of smart hydrogels has not been fully overviewed on the ground for drug delivery. In this study, a novel pH-sensitive smart hydrogel for drug delivery was investigated. Polyvinyl-alcohol (PVA) with polyacrylic acid (PAA) was blended adding synthetic hydroxyapatite (Hap) with freeze-thawed cycles and its effects were studied in terms of mechanical strength, bioactivity, and drug release profile. Mechanical strength towards compression tests was decreased after addition of Hap and storage modulus (G') increased. Bioactivity was confirmed after 14 days on simulated body fluid (SBF). Improvement of swelling and gel fraction with the addition of Hap throughout the polymer matrix. Moreover, a study was performed with theophylline-loaded samples for drug-delivery studies. Copyright © 2015 John Wiley & Sons, Ltd.**

**Keywords:** hydrogel composite; Poly(vinyl alcohol); nano hydroxyapatite; pH sensitive hydrogel

## INTRODUCTION

Recent scenarios on population aging worldwide estimates between 2000 and 2050 the proportion of people over 60 years will double from 11% to 22%, which means an increase from 605 million to 2 billion people.<sup>[1]</sup> In Western Europe, the population aged 65 or higher will increase to 27.3%, and China has already more than 10% of its population aged 65 and older.<sup>[2,3]</sup> With the population aging it gives rises to increase in diseases such as osteoporosis, cataracts, hypertension and cancer. In addition, the number of elderly and trauma patients requiring joint replacement or internal fixation is steadily increasing.<sup>[4]</sup> With these procedures, implant-related infections are the cause for revision surgery. The number of patients with such infections is rising owing to the lifelong risk for bacterial seeding on the implant.<sup>[5]</sup> Overall, about 5% of internal fixation devices become infected.<sup>[6]</sup> For this reasons, currently, the field of drug release in orthopedic applications is important.

A local release system of antibiotics from calcium phosphate-based ceramics coated titanium implants could be used to prevent post-surgical infections favoring early osteointegration of prostheses.<sup>[7,8]</sup> In addition, the calcium phosphate-based bioceramics, such as, hydroxyapatite (HAp) plays an excellent role in biomedical applications owing to their excellent biocompatible, osteoconductive and bioactivity properties, and its close chemical and physical resemblance to mineral component of bone tissue.<sup>[9]</sup> However, the incorporation of antibiotics in calcium-phosphate ceramics are extremely difficult.<sup>[10]</sup> The field of materials science has developed a number of alternative approaches to overcome these issues. There is a wide variety of materials available to address this challenge. An ideal material directed to this aim has to be: biocompatible, biodegradable, bioresolvable, bioactive, osteoconductive and osteoinductive.<sup>[11]</sup>

Moreover, porosity has to be added to the previously mentioned requirements in the case of 3D structures destined for implantation as porosity of the scaffold controls cell and blood vessel infiltration.<sup>[12]</sup> One type of materials with great potential in this is hydrogels. Poly(vinyl alcohol) (PVA) hydrogels have been proposed for a number of applications, especially in the biomedical areas for the preparation of heart valves<sup>[13,14]</sup> and pharmaceutical areas.<sup>[15]</sup> PVA, as a synthetic polymer, is able to form physically crosslinked hydrogels by a variety of methods, such as chemical crosslinking,<sup>[16]</sup> irradiation<sup>[17]</sup> or the freeze-thaw technique.<sup>[18]</sup> Polyvinyl alcohol hydrogels prepared using freeze/thaw techniques have great potential for biomedical applications as they do not contain solvent or other components which can increase the overall toxicity of the hydrogel.<sup>[15]</sup> Freeze/thawed gels are formed by freezing the polymeric solution. Upon freezing the solvent, crystals grow until they meet the facets of other crystals. The effect of these crystals is the formation of a porous system upon thawing.<sup>[19]</sup>

pH-sensitive hydrogels, such as polyvinyl alcohol coupled with polyacrylic acid (PAA), has been widely used in the area of drug-delivery systems.<sup>[20]</sup> pH-sensitive polymers consist of

\* Correspondence to: Michael J.D. Nugent, Athlone Institute of Technology, Materials Research Institute, Dublin Road, Co. Westmeath, Athlone, Ireland. E-mail: mnugent@ait.ie

<sup>†</sup> This article is published in *Journal of Polymers for Advanced Technologies in the special issue on Advanced Functional Polymers for Medicine 2015*, edited by Andreas Lendlein and Abhay Pandit.

a G. G. Lima, L. Campos, A. Junqueira, D. M. Devine, M. J. D. Nugent  
Athlone Institute of Technology, Materials Research Institute, Dublin Road,  
Co. Westmeath, Athlone, Ireland

b D. M. Devine  
The Mayo Clinic, Rochester, MN, USA

pendant acidic or basic group that either accept or release protons in response to changes in environmental pH. The applications of pH-sensitive hydrogels have already been reported.<sup>[21]</sup> However, one of the biggest draws of these hydrogels is their lack of bioactivity.<sup>[22]</sup> To overcome this problem, development of polymer composites is a major role in recent studies, because it can be tailored to any situation required. Consequently, ceramic hydrogels take up an important part on the field of drug delivery with biocompatibility and cell regeneration.

Hydrogels can improve their abilities by the addition of ceramics.<sup>[23,24]</sup> They can deliver *in situ* antibiotics to treat infections or growth factors to improve tissue regeneration. However, the field of ceramic/hydrogels composites still needs further investigation as this is a relatively new research area.<sup>[25,26]</sup> The investigation on pH sensitive hydrogel combined with nano hydroxyapatite (HAp) could prove beneficial in orthopedic applications. Therefore, in the current study polymeric/ceramic composites which utilizing PVA and PAA blends as the polymer matrix to provide elasticity, swelling capability and as a carrier vehicle for antibiotics, was combined with a synthesized HAp. This ceramic material was dispersed in the polymer matrix which was solubilized with water, and the final 3D construct was physically crosslinked using 10 cycles of freeze thawed (F/T).

## EXPERIMENTAL

### Materials

PVA, PAA, theophylline, SBF reagents and phosphate buffer saline (PBS) were supplied by Aldrich, Ireland. Pans used for DSC were obtained from TA instruments, Ireland.

### Nano hydroxyapatite synthesis

Hydroxyapatite was synthesized based on the work carried by<sup>[27]</sup> via wet chemical method using a slightly different concentration of 1.2 M  $\text{CaCl}_2 + 2 \text{ M } (\text{NH}_4)_2\text{HPO}_4$ .

### Polymeric composition formulation and fabrication of composites

Physically cross-linked (PVA) hydrogels were prepared by dissolving known concentrations of PVA, with average molecular weight of 4500 and a percentage of hydrolysis of 56–98% at 5% of concentration (w/v) in distilled water ( $\text{DH}_2\text{O}$ ), at 80°C with constant stirring until the complete solubilization of the PVA. Subsequently, nano hydroxyapatite (Hap) was dispersed in the polymer solution at 7 wt%, and finally PAA at different molecular weights (450,000 and 3,000,000) and concentrations (w/w) was added in the mixture at ambient temperature.

Once a homogeneous solution was produced a vacuum chamber was used for remove the remaining bubbles apparent on the samples solutions. Finally, the samples were rapidly frozen to constant temperature of  $-80^\circ\text{C}$  for 2 h. The frozen solutions were then thawed to an oven at  $25^\circ\text{C}$ . This procedure is performed either ten (10x) times as outlined in Table 1. For dried samples an oven was used for 24 h at  $30^\circ\text{C}$ .

### Scanning electron microscopy (SEM)

Composite morphology was observed using a Mira SEM (TESCAN Performance in Nanospace) in BSE mode using magnifications which ranged from 50 to 500x. The samples were sputtered with a gold using Baltec SCD 005 for 110 s at 0.1-mBar vacuum before testing. EDX analysis using Oxford instruments was used to confirm the elements composition of the composite components.

### Attenuated total reflectance Fourier transform infrared spectroscopy Fourier transform infrared (ATR-FTIR)

Attenuated total reflectance Fourier transform infrared spectroscopy was carried out on a Perkin Elmer Spectrum One fitted with a universal ATR sampling accessory. All data was recorded in the spectral range of  $4000\text{--}520\text{ cm}^{-1}$  utilizing four scans per sample cycle. Subsequent analysis was carried out using Spectrum software.

### Compression testing

Compression tests were performed on the Lloyd Lr10K, screw-driven testing machine fitted with a 2.5-kN load cell with a bespoke 30-mm diameter testing head. Hydrogels were evaluated as soon as they reach the dried state after the freeze/thawed. The hydrogel samples had a diameter of 30 mm and a thickness of 2.5 cm. Unconfined compression tests were carried out at a speed of 0.5 mm/min, and samples were strained to 50%. For both compression tests, a set of two samples were tested per batch.

### Rheological measurements

Rheology tests were carried out using an AR 1000 rheometer from TA instruments. The tests were carried out using the parallel plate method. A Peltier plate was used as the frequency sweep test. A 20-mm steel plate was used as the top geometry. A low frequency and low strain range was adopted. A strain sweep was applied from  $1.8\text{E}^{-4}$  to  $1\text{E}^{-3}$  at a frequency of 1 Hz. A frequency sweep was applied at a range of 0.1–100 Hz. In all cases a compression load of  $2 \pm 0.5 \text{ N}$  was exerted on the swollen hydrogels during testing, and data is presented as mean of two measures.

**Table 1.** Summary of the polymeric–ceramic samples prepared (%wt)

Sample code	Hap	PAA low M.W.	PAA high M.W.	Sample code	Hap	PAA low M. W.	PAA high M.W.
PVA	0	0	0	7Hap	7	0	0
0Hap5L	0	5	0	7Hap5L	7	5	0
0Hap30L	0	30	0	7Hap30L	7	30	0
0Hap5H	0	0	5	7Hap5H	7	0	5
0Hap30H	0	0	30	7Hap30H	7	0	30
0Hap50H	0	0	50	7Hap50H	7	0	50
0Hap90H	0	0	90	7Hap90H	7	0	90

## Swelling behavior

Swelling studies of the composite samples were carried out using buffer solution at pH 7.4. For the swelling properties, the PVA hydrogels was measured gravimetrically.<sup>[28]</sup> To measure the swelling kinetics, the pre-weighted samples were immersed in distilled water. The excess surface water was gently removed with paper and the swollen samples were weighted at various time intervals. The swelling ratio percentage of a hydrogel can be defined as:

$$S(\%) = (W_s - W_d)/W_d \times 100 \quad (1)$$

where  $S(\%)$  represents the weight of the swollen hydrogel at an specific time, also known as water uptake content, and  $W_d$  is the hydrogel dried mass before beginning the swelling studies.

## Gel content

Gel content values were measured by after the samples reached swelling equilibrium on swelling behavior tests. The samples were then taken out and dried in a vacuum oven at 60°C until the weight of the sample was constant. The gel content was calculated using the following formula:

$$\text{Gel Fraction}(\%) = (W_{ex}/W_o) \times 100 \quad (2)$$

where  $W_{ex}$  is the final weight of the sample after swelling and drying and  $W_o$  is the initial weight of the sample before the experiment.

## Drug dissolution studies

Drug dissolution profiles were obtained using a Sotax AT7 smart dissolution system from Carl Stuart Ltd. The hydrogels were

loaded with 5 wt% of theophylline cylindrical samples and tested in phosphate buffer solution of pH 7.4 at 37°C. The stir rate was set to 100 rpm with 900 ml of dissolution media used per vessel. Six vessels were used for each scan. Samples were automatically taken at set intervals and analyzed by ultraviolet (UV) light on a PerkinElmer lambda 2 spectrometer. Two samples of each batch from Table 1 hydrogels with 5% theophylline incorporated were analyzed, and the software produced a plot of the average release.

## Bioactivity

For the bioactivity test it was used simulated body fluid solution (SBF) of Kokubo,<sup>[29]</sup> according to the preparation protocol and methodology applied.<sup>[29]</sup> Each sample was placed in a falcon tube containing 50 ml of SBF solution, and then placed in the heat bath at 37°C for a period of 14 days. After the set period of immersion, the samples were washed in distilled water and brought to the oven for drying at 40°C for 24 h. The degree of bioactivity was qualitatively estimated observing the sample surface. The bioactivity of the response is observed by the presence of hydroxyapatite on the samples, which can be detected by SEM/EDS.

## RESULTS

### Hydrogel morphology

SEM analysis was used to visualize the hydroxyapatite dispersion in the matrix and overall morphology of the composite. PVA hydrogels formed by freezing and thawing are strong and flexible. Because of difficulties in sample preparation, the

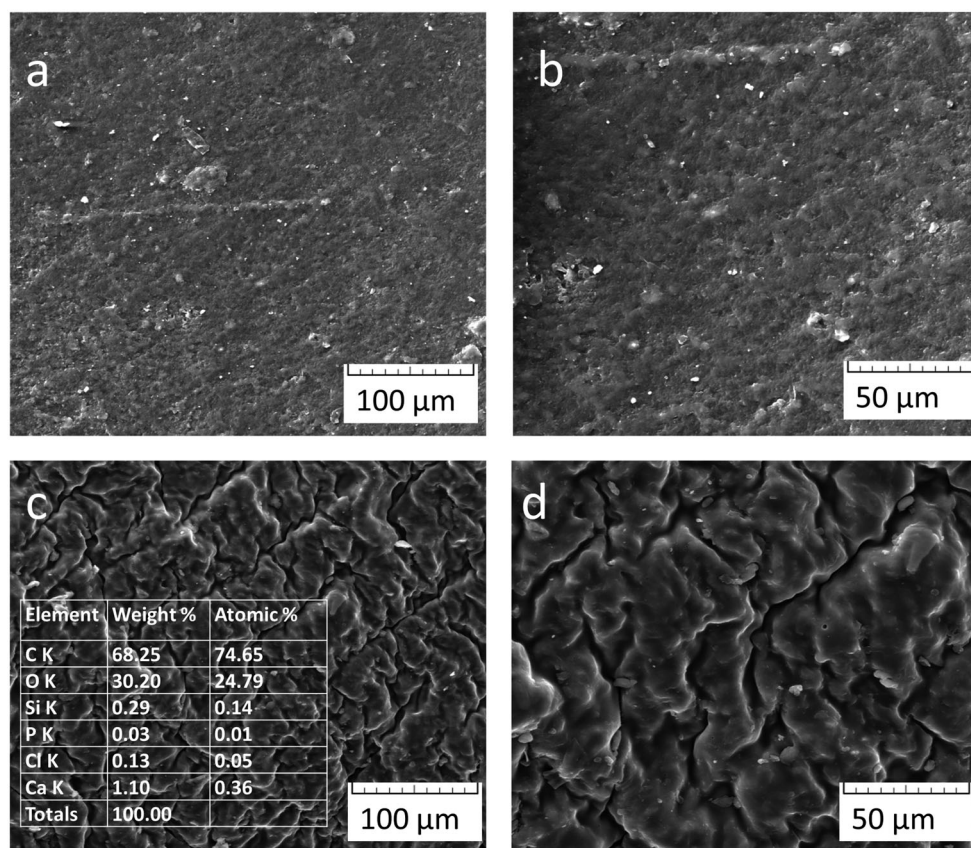


**Figure 1.** SEM images of the hydrogels: 0Hap50H (a) 500x and (b) 1kx; 7Hap50H (c) 500x and (d) 1kx.

hydroxyapatite maximum concentration possible to disperse in the polymer matrix in all experienced conditions achieved was seven percent (w/w). The morphologies of the composites investigated in this study can be observed in Fig. 1. With the addition of the hydroxyapatite it can be observed that a new layer is formed throughout the polymer. Furthermore, the Hap was well dispersed all over the hydrogel matrix because no aggregates of this ceramic were observed on these surfaces. In addition, a highly porous hydrogel can be noted. Moreover, from the Table 1 the Hap components calcium (Ca) and phosphorus (P) were identified on the hydrogel which confirms the incorporation of the Hap.

ATR-FTIR analysis of PVA/Hap/PAA hydrogels.

The ATR-FTIR spectra for PVA, PVA + Hap and PVA + Hap + PAA hydrogels are illustrated in Fig. 2; the region is zoomed in the range of 2000–600  $\text{cm}^{-1}$  since it has the most significant changes in the present study. The synthesized hydroxyapatite characteristic phosphate group peaks were observed at 1027  $\text{cm}^{-1}$  (corresponding to  $\text{PO}_4^{3-}$   $\nu_3$  stretching) and 962  $\text{cm}^{-1}$  (associated with  $\text{PO}_4^{3-}$   $\nu_1$  stretching).<sup>[30]</sup> Synthesis of pure hydroxyapatite was confirmed by the complete reaction of constituents by the absence of any calcium carbonate groups between 1400 and 1500  $\text{cm}^{-1}$ . In terms of the hydrogel matrix, the polyvinyl alcohol and polyacrylic acid peaks are generally correspondent to alcohol and carboxylic acid groups. With addition of PAA some of the peaks become more defined and more intense based on the concentration of the PAA presented in the hydrogel. In addition, new bands were observed corresponding solely to PAA between 1750 and 1710  $\text{cm}^{-1}$  which are characteristic bands of C=O and C—O stretching of carboxylic groups.<sup>[31,32]</sup> The peak at 1640  $\text{cm}^{-1}$  can be assigned to the C=O stretching and hydrogen

bonding coupled with  $\text{COO}^-$  stretching.<sup>[21,33]</sup> As PVA only shows a small intensity peak at 1641  $\text{cm}^{-1}$  because of the water absorption, the increase in the intensity of the peak at about 1630  $\text{cm}^{-1}$  indicates the improvement of PVA/Hap hydrogel. In addition, the peak around 1027  $\text{cm}^{-1}$  only shows on hydrogels after the addition of Hap, and it is more evident on pure PVA + Hap. Adding PAA to the PVA + Hap the peak around 1027  $\text{cm}^{-1}$  is merged with the 1089  $\text{cm}^{-1}$ .

### Mechanical analysis of the hydrogel systems

In the rheology measurements, samples were tested in duplicate. The average value of the storage modulus data for each type of hydrogel was calculated and results are shown in Fig. 3a and c. With the addition of the Hap on pure PVA no apparent differences were observed. However, hydrogels with PAA + Hap presented higher values of storage modulus in comparison to the samples without Hap. Moreover, hydrogels loaded with Hap containing PAA with low M.W. had visual minor changes in comparison to higher M. W. For the frequency-sweep tests, Hap seems to have a huge factor on their values of storage modulus. The samples containing Hap + PAA had slower decrease rates of storage modulus as the frequency increases, which confirms the improvement of Hap over these samples. Furthermore, the samples with higher concentrations of PAA had the maximum values of storage modulus. However, hydrogels with low M.W. of PAA had their values decreased with the addition of Hap, and no apparent difference was observed on the pure PVA. With the addition of Hap the  $G'$  of 7Hap90H significantly increased to 4200 Pa. The significant enhancement in ultimate strength appeared with increasing the concentration of the hydrogels containing

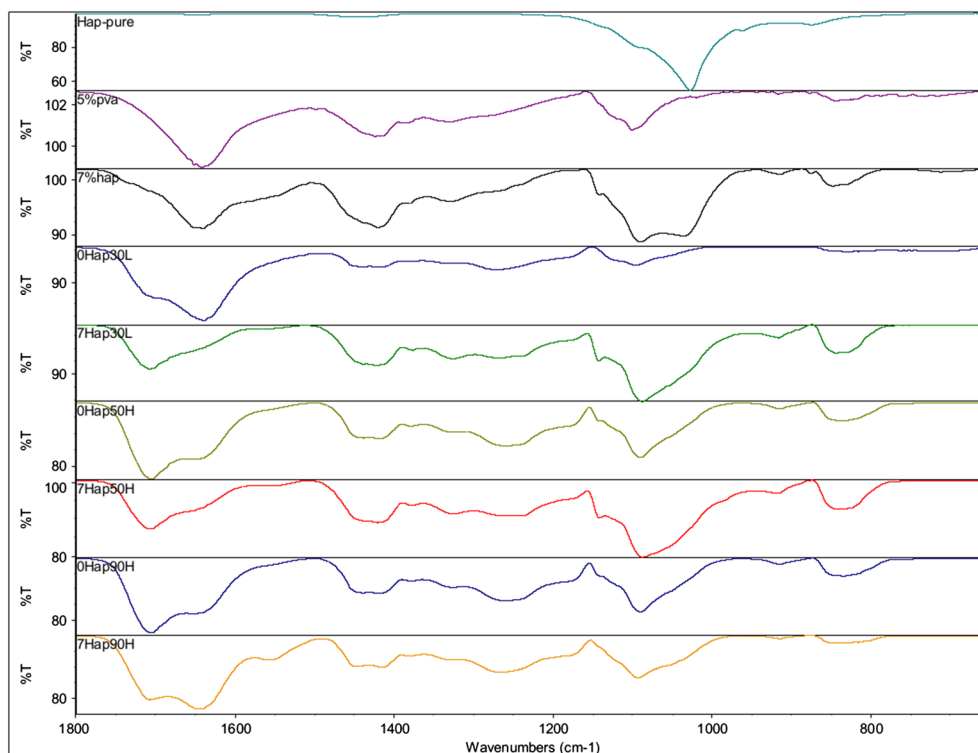
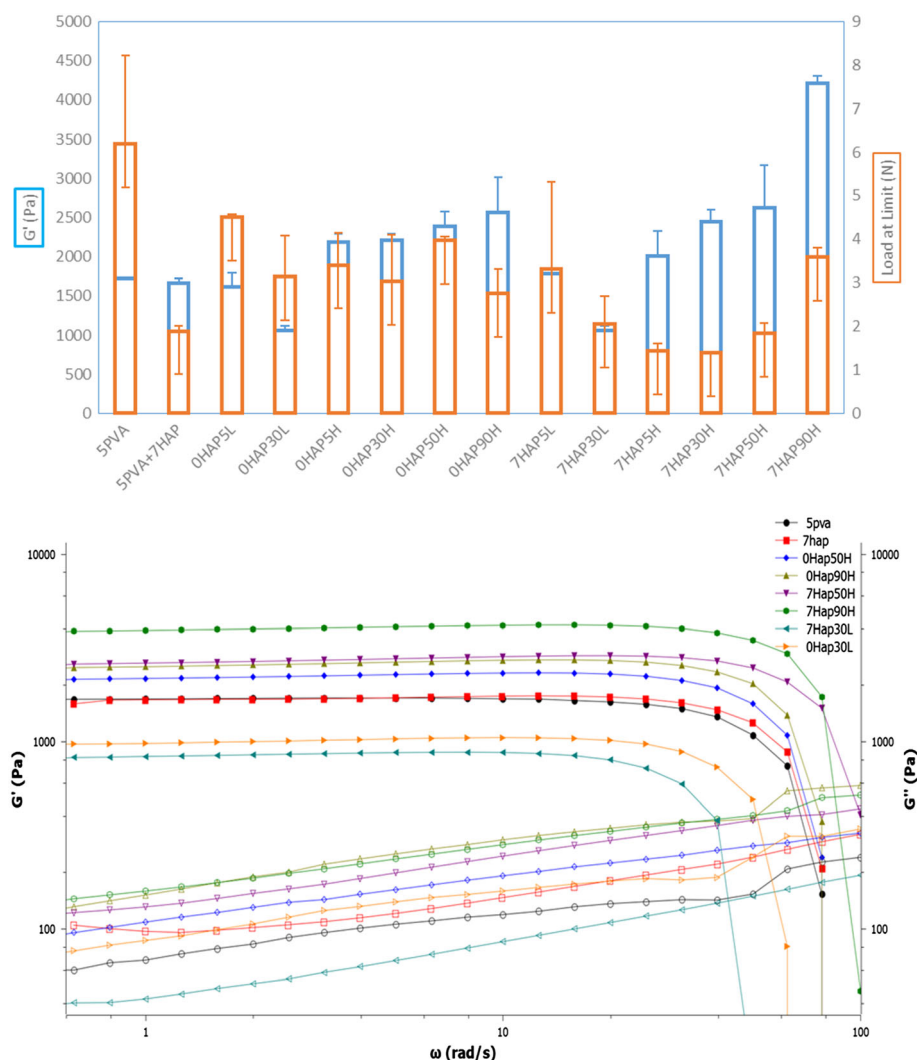


Figure 2. FTIR spectra of the Hap, matrix and various composites studied.





**Figure 3.** (Top) Blue: Strain-sweep tests from composites with and without Hap. Orange: Compression tests from composites with and without Hap. (Bottom) Frequency sweep tests for the studied samples.

PVA+PAA with 10× of F/T, which is confirmed by some authors.<sup>[21,34]</sup> Results for unconfined compression tests are listed in Fig. 3b. Unconfined compression tests revealed that the incorporation of Hap into the hydrogel caused a decrease in their loads at limit; values for PVA,  $0.06 \pm 0.02$  MPa, were significantly higher than for 7Hap,  $0.019 \pm 0.001$  MPa.

### Swelling, polymer fraction and drug release studies

Figure 4 presents the data for the swelling, polymer fraction and drug release studies. All the samples were swelled, and two different equilibria were achieved; samples with lower concentration of PAA showed the equilibrium within 8 h, and samples with higher concentration of PAA achieved the equilibrium after 24 h. However, within 6 h 80% of their maximum swelling was completed indicating that this hydrogel has fast swelling characteristics. A further increase occurs for the PVA hydrogel with the addition of Hap. In the case of blends, the swelling ratio increased with increase in PAA content in the blend because of the extensive swelling of PAA facilitated by the carboxylic acid

groups. When Hap is presented in the polymer matrix, the maximum values of the swelling ratio are increased for most of the conditions. In addition, the swelling ratio raised faster. The polymer fractions calculated for the PVA/Hap hydrogels are shown in Fig. 4b. Hap were found to enhance the polymer fraction in hydrogel. The polymer fraction significantly increased from 24% for PVA hydrogel to 26% and 7.5% for 0Hap50H to 10% with the addition of Hap. Finally, Fig. 4c shows the results obtained from drug dissolution studies carried out on PVA/PAA hydrogels with 5% theophylline incorporated. The drug release mechanisms in swellable hydrogels have been widely reported.<sup>[35,36]</sup> Before swelling occurs the drug molecules are entrapped within the polymer matrix. As the hydrogel swells, the mesh size becomes larger and then allows the drug molecules to be free to diffuse out of the gel. In addition, the gels in this research are partially swollen upon synthesis, and therefore drug molecules are free to diffuse out without further swelling. However in the basic media of pH 7.4 the gels swell to a greater extent allowing more ease for solute diffusion. Therefore drug release occurs because of a combination of macromolecular relaxations because of swelling. Comparing

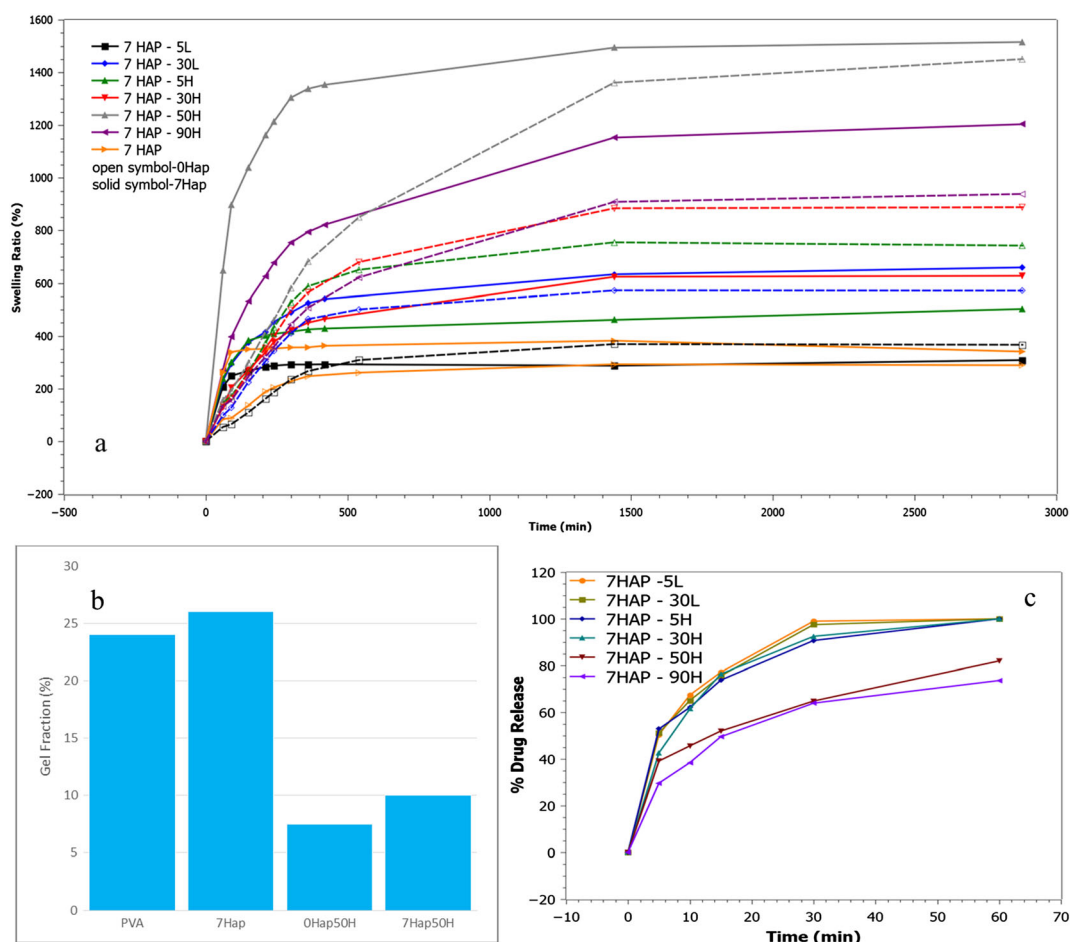


**Figure 4.** (a) Swelling studies for the Hap hydrogels. (b) Gel fraction for PVA; 7Hap; 0Hap50H and 7Hap50H. (c) Drug release studies for the samples with Hap loaded with theophylline.

the drug release with the swelling studies it is evident that it follows the same tendency. Furthermore, samples with lower concentration of PAA release quicker the drug than samples with higher concentration.

## Bioactivity

*In vitro* bioactivity tests were performed using simulated body fluid (SBF) leaving the samples for 14 days at 37°C. Figure 5

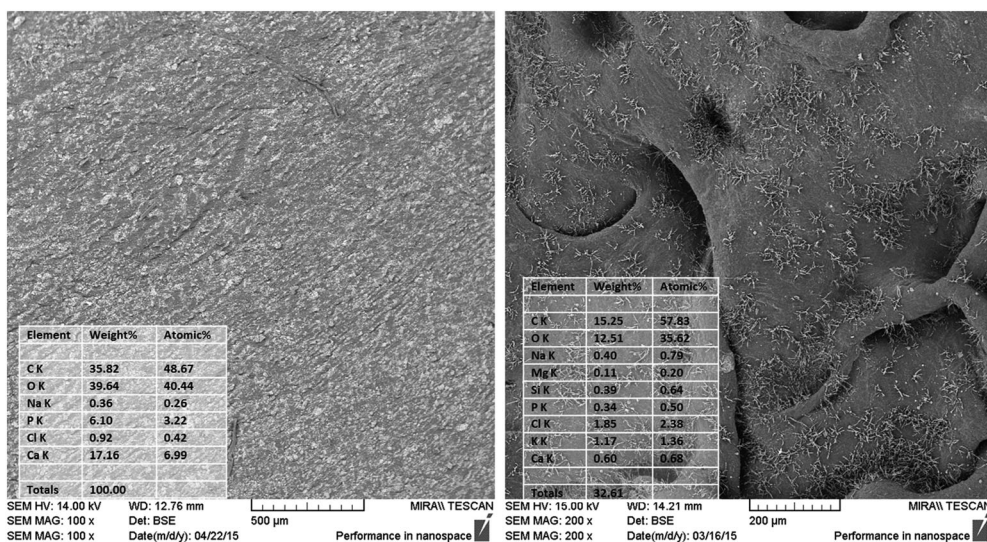


**Figure 5.** SEM micrographs showing the morphology after testing in SBF for 14 days for the samples: (a) 7Hap and (b) 7Hap50H with respective EDS of each sample.

shows the images taken by SEM surface of the studied samples. A new layer was formed on the surface of the samples containing Hap which shows a porous morphology on 7Hap samples and in the case of 7Hap50H samples, the layer does not present a globular morphology. Analyses carried out to determine the elements presented in this new layer are shown in the EDS spectra. It is observed that the two surfaces contain calcium and phosphorus, calcium phosphate thus formed on the hydrogel. Similar morphologies have been reported in the literature.<sup>[27,37]</sup>

The values of Ca and P given by EDS were determined to Ca/P ratio, and these values were 2.1 and 1.76.

## DISCUSSION

Hydroxyapatite comprises the mineral phase of bone, and it also readily heals into bone and fuses with it.<sup>[9]</sup> Prevention of post-surgical infections, pain and inflammation is a challenge problem in orthopedic surgery but might be improved by using a local release system of drugs/antibiotics. Coatings based on calcium phosphate have shown to enhance early bone apposition and long-term fixation of prostheses. However, this osteo integration process could be disadvantaged by the presence of bacteria in the peri-implant bone healing area.<sup>[10]</sup> Hence, combinations of materials, i.e. the good biocompatibility of hydroxyapatite mixed with the drug release properties of hydrogels could enhance the abilities and be effective. In the current study the polymer phase utilized is a PVA-PAA blend poly(vinyl alcohol)/poly (acrylic acid) (PVA/PAA) and is a well-known blend system for its molecular level miscibility through inter-polymer hydrogen bond interactions.<sup>[21,37]</sup> The nano hydroxyapatite was selected because of its bone-bonding property and high binding affinity for a variety of pharmacological substances such as antibiotics, drugs, etc.<sup>[10,38]</sup>

The morphologies of the hydrogels were observed in SEM in their dehydrated form; it was noticed that a new layer formed on the surface of these hydrogels with Ca and P components indicating the incorporation of HAp on these samples. Higher values of ceramic in the composite appeared to produce a higher level of interconnectivity in the porous structure.

The slight difference in the structural changes as observed using FTIR can be induced by the effect of HAp, which can influence the adhesion in the hydrogels<sup>[39]</sup> which then leads to reinforcement of intermolecular and intramolecular bonds. It was noted that hydrogels with HAp-ceramic content had more bands than the ones without. The peak resolution at  $1690\text{ cm}^{-1}$  reduced with increase in PVA content in the blend which indicates the formation of new intermolecular interaction between PVA and PAA at the expense of cyclic dimers. With the incorporation of the hydroxyapatite component this intermolecular bonding appears to have reduced in preference to the formation of intramolecular bonds between the Hap material and the carboxylic group of PAA as evidenced by the formation of a peaks in the region of  $1027$  to  $962\text{ cm}^{-1}$  both of which are indicative of hydrogen bonding of the carboxylic group of PAA. Samples with low M.W. of PAA had the most significant difference. Because of its dense chains more intramolecular bonds had to be forfeited for the carboxylic group of PAA and Hap. Furthermore, this increase in intramolecular bonding appeared to interfere with the crystallization of the PVA phase of the composite as evidenced by the reduction in the peak at  $1140\text{ cm}^{-1}$

which corresponds to crystalline PVA. Similar findings were obtained in literature<sup>[40,41]</sup> that the incorporation of calcium into the PVA reduced the intermolecular bonding of the polymer giving preference to intramolecular bonding with calcium.

The mechanical properties of these hydrogels indicate a decrease on compression because of incorporation of Hap, which could have happened because the hydroxyapatite disrupted the crosslinks between monomeric chains and thus causes the polymeric chains to have fewer opportunities to covalently link to the network.<sup>[37]</sup> On the other hand, values of rheology show an increase on storage modulus with increasing the PAA concentration on Hap hydrogels. Frequency-sweep analysis indicates that the composites behave like a solid as indicated by the storage modulus response which was higher than the corresponding loss modulus. This is a characteristic feature of crosslinked hydrogel.<sup>[42]</sup> In this work the maximum  $G'$  recorded was approximately 30 KPa. These results correspond favorably with the results from other studies where composite materials were assessed for bone regeneration applications, and their storage modulus values were reported to be between 300 Pa and 15 KPa.<sup>[43]</sup> In addition, frequency-sweep tests which show the increase  $G'$  because of Hap for high M.W. of PAA can be explained with the FTIR because of its interconnect bonds. In summary, these results indicate that with the incorporation of Hap the material becomes brittle decreasing the strength of the material but increases its storage modulus.

Swelling analysis of the composites indicated that the composites swelled more than the matrix alone.<sup>[44]</sup> reported a similar phenomenon because of the incorporation of  $\text{Ca}^{2+}$  and  $\text{Mg}^{2+}$  ions which were shown to increase swelling. Furthermore, samples with higher content of PAA and incorporated with Hap on their matrix had higher values of swelling in comparison to samples with lower content of PAA. This might be owing to intramolecular bonds between the HAp and PAA which increases with more PAA concentration. Samples without HAp had a slower swelling rate; this might have happened because of the higher level of crosslink with hydrogen bonds. The samples had a slower rate of swelling because it is hard for the relaxation walls to absorb water owing again to their interconnect bonds by the crosslink. In these samples, the watery media needed increased time to penetrate the inside of the sample and fill the pores. Furthermore, electrostatic repulsion and crosslink disruption favor the increase in swelling ratio observed for hydrogels.<sup>[44]</sup> Nevertheless, the HAp hydrogels with lower concentration of PAA had a reduction in swelling which seems to indicate that this electrostatic repulsion has been overcome with intramolecular bonding. The increase in gel fraction was associated with the hydroxyapatite crosslinks between polymeric chains of PAA. The gel fraction in general was slightly increased in all hydrogels. The drug release studies showed that Hap hydrogel samples with lower concentrations of PAA released completely the drug in 60 min while when increasing its contents of PAA the release rate is somewhat lowered. These findings for swelling, gel fraction and drug released agree with literature.<sup>[21,34,45]</sup>

The bioactive properties of the hydrogel were studied *in vitro* by analyzing the ability of the scaffold to form an apatite layer when placed in simulated body fluid (SBF). Polymers, have very limited if any bioactive surface properties because of their low protein absorption.<sup>[37]</sup> With the addition of Hap on the hydrogels, a bioactive surface was achieved. From the EDS results the ratio Ca/P achieved was higher than 1.63 which is a similar calcium phosphate compound from natural Hap.



## CONCLUSIONS

In this work we have evaluated the potential for novel PVA/PAA/HAp composites fabricated using the F-T process for use as a bone healing and drug delivery applications. The results of the study indicate that properties of the composite were dependent on the intermolecular and intramolecular bonding between the different components in the composite, and this could be controlled by varying the concentration and composition of the different components. Furthermore, samples were placed in SBF for 14 days as biomineralization studies. The apatite layer was observed only in the presence of nano HAp. These results indicate that the composite developed in the current study has enormous potential as a drug delivery carrier in orthopedic applications.

## REFERENCES

- [1] K. Jin, J. W. Simpkins, X. Ji, M. Leis, I. Stambler, *Aging Dis.* **2015**, 6(1), 1–5.
- [2] A. Peine, A. Faulkner, B. Jæger, E. H. M. Moors, *Technol. Forecast. Soc. Change* **2015**, 93, 1–9.
- [3] J. H. Flaherty, M. L. Liu, L. Ding, B. Dong, Q. Ding, X. Li, S. Xiao, *J. Am. Geriatr. Soc.* **2007**, 55, 1295–1300.
- [4] A. Trampuz, A. F. Widmer, *Curr. Opin. Infect. Dis.* **2006**, 19(4), 349–356.
- [5] W. Zimmerli, A. Trampuz, P. E. Ochsner, *New Engl. J. Med.* **2004**, 351(16), 1645–1654.
- [6] R. O. Darouiche, *New Engl. J. Med.* **2004**, 350(14), 1422–1429.
- [7] Q. Z. Chen, C. T. Wong, W. W. Lu, K. M. C. Cheung, J. C. Y. Leong, K. D. K. Luk, *Biomaterials* **2004**, 25(18), 4243–4254.
- [8] D. Park, I. Kim, H. Kim, A. H. K. Chou, B. Hahn, L. Li, S. Hwang, *J. Biomed. Mater. Res. B Appl. Biomater.* **2010**, 94(2), 353–358.
- [9] X. Xiao, R. Liu, C. Chen, L. Huang, *J. Mater. Sci. Mater. Med.* **2008**, 19(2), 797–803.
- [10] M. Stigter, J. Bezemer, K. De Groot, P. Layrolle, *J. Control. Release* **2004**, 99(1), 127–137.
- [11] M. P. Staiger, A. M. Pietak, J. Huadmai, G. Dias, *Biomaterials* **2006**, 27, 1728–1734.
- [12] V. Karageorgiou, D. Kaplan, *Biomaterials* **2005**, 26(27), 5474–5491.
- [13] W. K. Wan, G. Campbell, Z. F. Zhang, A. J. Hui, D. R. Boughner, *J. Biomed. Mater. Res.* **2002**, 63(6), 854–861.
- [14] H. Jiang, G. Campbell, D. Boughner, W.-K. Wan, M. Quantz, *Med. Eng. Phys.* **2004**, 26(4), 269–277.
- [15] C. M. Hassan, N. A. Peppas, *Adv. Polym. Sci.* **2000**, 153, 38–65.
- [16] C. R. Nuttelman, D. J. Mortisen, S. M. Henry, K. S. Anseth, *J. Biomed. Mater. Res.* **2001**, 57(2), 217–223.
- [17] R. H. Schmedlen, K. S. Masters, J. L. West, *Biomaterials* **2002**, 23(22), 4325–4332.
- [18] R. Langer, N. A. Peppas, *AIChE J.* **2003**, 49(12), 2990–3006.
- [19] A. Kumar, A. Srivastava, I. Y. Galaev, B. Mattiasson, *Prog. Polym. Sci. Oxford* **2007**, 32, 1205–1237.
- [20] C. A. Schoener, H. N. Hutson, N. A. Peppas, *Polym. Int.* **2012**, 61(6), 874–879.
- [21] J. Jose, F. Shehzad, M. A. Al-harhi, *Polym. Bull.* **2014**, 71(11), 2787–2802.
- [22] J. Zhu, *Biomaterials* **2010**, 31(17), 4639–4656.
- [23] Y. Dai, H. Liu, B. Liu, Z. Wang, Y. Li, G. Zhou, *Ceram. Int.* **2015**, 41(4), 5894–5902.
- [24] W. Togami, A. Sei, T. Okada, T. Taniwaki, T. Fujimoto, S. Tahata, K. Nagamura, Y. Nakanishi, H. Mizuta, *J. Biomed. Mater. Res. B Appl. Biomater.* **2015**, 103, 188–194.
- [25] S. Van Vlierberghe, P. Dubruel, E. Schacht, *Biomacromolecules* **2011**, 12(5), 1387–1408.
- [26] W. Li, M. Pastrama, Y. Ding, K. Zheng, C. Hellmich, A. R. Boccaccini, *J. Mech. Behav. Biomed. Mater.* **2014**, 40, 85–94.
- [27] R. Murugan, S. Ramakrishna, *Biomaterials* **2004**, 25(17), 3829–3835.
- [28] C. Yang, L. Xu, Y. Zhou, X. Zhang, X. Huang, M. Wang, Y. Han, M. Zhai, S. Wei, J. Li, *Carbohydr. Polym.* **2010**, 82(4), 1297–1305.
- [29] T. Kokubo, H. Takadama, *Biomaterials* **2006**, 27(15), 2907–2915.
- [30] P. Jongwattanapisan, N. Charoenphandhu, N. Krishnamra, J. Thongbunchoo, I.-M. Tang, R. Hoonsawat, S. M. Smith, W. Pon-On, *Mater. Sci. Eng. C* **2011**, 31(2), 290–299.
- [31] J. J. Maurer, D. J. Eustace, C. T. Ratcliffe, *Macromolecules* **1987**, 20, 196–202.
- [32] S. Nesrinne, A. Djamal, *Arab J. Chem.* **2013**; (in press). doi: 10.1016/j.arabj.2013.11.027
- [33] J. H. Muyonga, C. G. B. Cole, K. G. Duodu, *Food Chem.* **2004**, 86(3), 325–332.
- [34] M. J. McGann, C. L. Higginbotham, L. M. Geever, M. J. D. Nugent, *Int. J. Pharm.* **2009**, 372(1–2), 325–332.
- [35] M. D. Kurkuri, T. M. Aminabhavi, *J. Control. Release* **2004**, 96(1), 9–20.
- [36] Y. Qiu, K. Park, *Adv. Drug Deliv. Rev.* **2012**, 64, 49–60.
- [37] J. A. Killion, L. M. Geever, D. M. Devine, H. Farrell, C. L. Higginbotham, *Int. J. Polym. Mater. Polym. Biomat.* **2014**, 63(13), 641–650.
- [38] D. J. A. Netz, P. Sepulveda, V. C. Pandolfelli, A. C. C. Spadaro, J. B. Alencastre, M. Bentley, J. M. Marchetti, *Int. J. Pharm.* **2001**, 213(1), 117–125.
- [39] J. H. Priya, R. John, A. Alex, K. R. Anoop, *Acta Pharmaceutica Sinica B* **2014**, 4(2), 120–127.
- [40] J. S. Gonzalez, V. A. Alvarez, *J. Mech. Behav. Biomed. Mater.* **2014**, 34C, 47–56.
- [41] S. El-Sayed, K. H. Mahmoud, A. A. Fatah, A. Hassen, *Physica B Condens. Matter* **2011**, 406(21), 4068–4076.
- [42] D. Calvet, J. Y. Wong, S. Giasson, *Macromolecules* **2004**, 37(20), 7762–7771.
- [43] J. A. Killion, S. Kehoe, L. M. Geever, D. M. Devine, E. Sheehan, D. Boyd, C. L. Higginbotham, *Mater. Sci. Eng. C Mater. Biol. Appl.* **2013**, 33(7), 4203–4212.
- [44] V. B. Bueno, R. Bentini, L. H. Catalani, D. F. S. Petri, *Carbohydr. Polym.* **2013**, 92(2), 1091–1099.
- [45] Y. Liu, L. M. Geever, J. E. Kennedy, C. L. Higginbotham, P. A. Cahill, G. B. McGuinness, *J. Mech. Behav. Biomed. Mater.* **2010**, 3(2), 203–209.